Advances in Physics Theories and Applications
ISSN 2224-719X (Paper) ISSN 2225-0638 (Online)
Vol.60, 2016
www.iiste.org

Effect of Fuel on the Structural and Optical Properties of MgO Nanoparticles Prepared by Auto–Combustion of Sol-Gel Method

Ziad T. Khodair*, Tagreed M. Al – Saadi** , Ahmed H. Abed*

* Diyala University / College of Science / Physics Dep.

** Baghdad University / College of Education for Pure Sciences - Ibn Al-Haitham / Physics Dep.

Abstract

Magnesium nitrate as precursor and citric acid as fuel are used as a starting material for the preparation magnesium oxide (MgO) nanoparticles via sol- gel of auto–combustion method. X-ray diffraction patterns indicate that the obtain (MgO) nanoparticles are in good crystallinity and show that the all grain size was decreases with increasing of concentration citric acid as fuel. The crystallite size was calculated using Scherrer and Williamson-Hall formula at difference ratios of fuel which have maximum crystallite size (13.55 nm) and (14.26 nm) respectively. The SEM images for MgO powder prepared with fuel (Citric acid) at three various molar ratios show the morphology of the oxides is mostly spherical with some agglomeration. The optical properties show that the transmittance decrease with increase the fuel amount and additives ammonia and fuel played an important role in the combustion.

Keywords: MgO , Nanoparticles , Sol-Gel, Auto–Combustion, Structural , Optical

1.0. Introduction

Magnesium oxide is an important oxide mineral that used in many applications such catalyst supports, catalysis, toxic wastes remediation, adsorbents, absorbent for many pollutants and refractory materials (Jiahai, Fantao, Chuncheng, Yunxia, Huihui. & Juncheng, L. 2011). Thus many wide studies have been executed to synthesis nanoscale MgO powders using different novel wetly chemical methods, e.g. Sol-Gel synthesis, followed by spray pyrolysis and supercritical drying (G. Dercz, K. Prusik, L. Pajaki , R. Pielaszek , J. J. Malinowski , & W. Pudlo. 2009). MgO is synthesized by the disintegration of different magnesium salts in air. However, the MgO particles generative by this method are usually large size and irregular with low specific surface area. MgO NPs with narrow size distributions can be prepared by using various chemical methods , the oxide particle sizes and morphology are dependent on such, temperature of precipitation, preparation conditions as the pH, calcination temperature/time and concentration or ionic strength (V. S tengl , S. Bakardjieva, M. Mar kova , P. Bezdic ka, & J. S ubrt . 2003). It can be prepared in widely different shapes and particle sizes .It has been documented that the size and shape of nanocrystalline magnesium oxide particles awarded them with high reactivity and specific surface, because of the structural defects on their surface high and concentration of edge/corner sites (Zhen-Xing Tang , & Lu-E Shi. 2008)..

In this work, MgO nanoparticles were synthesized via sol- gel of Auto – Combustion process using citric acid as fuel. In addition to study effects of fuel to optical properties, crystal structure, and crystalline size. The optical properties of MgO nanoparticles samples were investigated by (UV-Visible1800) spectrophotometer.

2.0. Experimental method

Magnesium oxide nanoparticle were prepared by sol gel auto-combustion method, using magnesium nitrate hexahydrate [Mg(NO_3)$_2$. 6(H_2O)], and citric acid ($C_6H_8O_7$. H_2O) as a fuel. A stoichiometric amount of magnesium nitrate and citric acid were dissolve in deionized water at 90^{o}C with magnetic starrier. Five samples of fixed molar ratios of magnesium nitrate to citric acid such as (1:0.5, 1:0.6, 1:1, 1:1.75 and 1:2) were prepared and these five samples will be named as P_1, P_2, P_3, P_4 and P_5 respectively. The pH of the solutions thus get to resulted (7). The white color solutions where allowable to steaming on a preheat plate preserving the solution temperature at 70-90°C where the gel started to form. A sudden elevate of the temperature to (200°C) allowed to form the gels as MgO powders. Finally, the powders was calcined at 600°C for (2 h) to get to MgO nanoparticle.

3.0. XRD analysis

Figure (1) shows the XRD modes of the five samples synthesized by solution combustion process off the redox mixtures with fuel ratios equal to (1:0.5, 1:0.6, 1:1, 1:1.75 and 1:2), respectively. As presented in Figure (3), the characteristic peaks of powders corresponding with (MgO, JCPDS 45-0946), reveal that the main crystal phase of the combustion synthesized powders. Moreover, the characteristic peaks becomes stronger and sharper when fuel ratio 0.5, which refers that MgO are better naonscale size, which were calculated according to the Scherrer and Williamson-Hall formula and listed in table (1), which is markedly decreased when the fuel ratio increases. In spite the five samples all subjected to heat treatment at 600 °C for 2 h, their difference in crystalline size and crystallization could be mainly attributed to the combustion process (fuel amount). Additives ammonia and fuel played an important role in the combustion. The structural, crystallite size and morphology are affected by the mole ratios of fuels-to-nitrates. (G. Mahmoudzadeh, S. A. Khorrami, S. S. Madani & M. Frounchi . 2012).

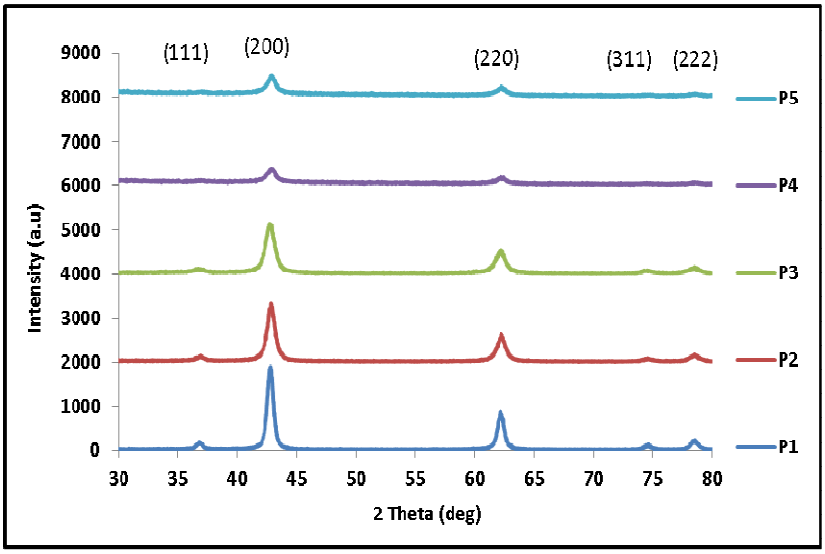

Figure 1. XRD patterns of the combustion synthesized products from the precursors with fuel equal to P_1)1: 0.5 , P_2) 1:0.6 , P_3) 1 : 1 , P_4) 1 : 1.75 and P_5) 1 : 2, respectively.

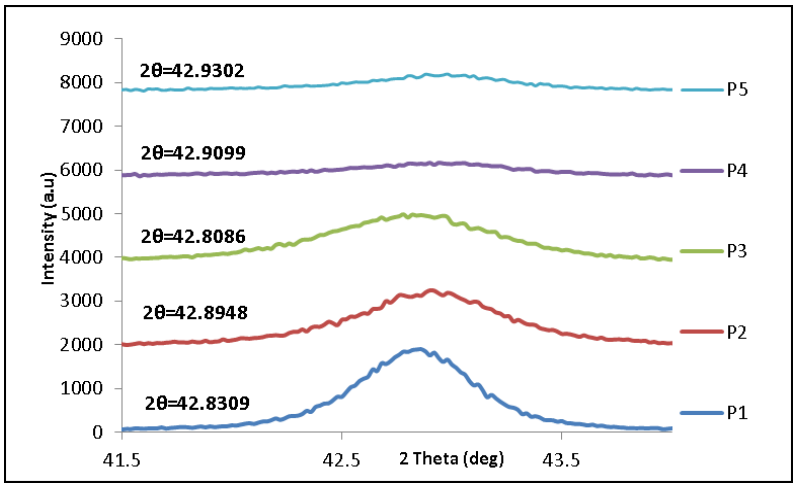

Figure 2. XRD data of the (200) peak.

As the concentration of citric acid changes the peak (200) changes dominantly the peak (002) of each the samples are drawn in Fig (2). was increase in concentration citric acid cause decrease in intensity. This shifting in peak position and decrease in intensity reflect that the presence of impurities resulting from spontaneous combustion process, which leads to a decline in the intensity of the peaks of the magnesium oxide and the best sample(P_1) is because it has the highest peaks and this shows they do not contain impurities(Y. T. Prabhu, K. Venkateswara Rao, V. Sesha Sai Kumar, & B. Siva Kumari. 2013).

3.1. B. Crystallite Size Calculation

The lattice strain and crystallite size induced in powders appearing from defects like distortion, imperfection, twinning, and dislocation was determined by Williamson-Hall equation and Scherrer formula as follows (Nabeel A. Bakr, Ziad T. Khodair & Israa A. Alghalabi. 2015). M. J. S. Mohamed, & N. Selvakumar, 2012).

$D = K\lambda / \beta \cos\theta$ …... (1)

$\beta_{hkl}\cos\Theta = (K\lambda / D) + (4\varepsilon \sin\Theta)$ ……(2)

where, K: constant, λ: wavelength of Cu kα radiation D: crystallite size. W-H plot is shown in figure (3).

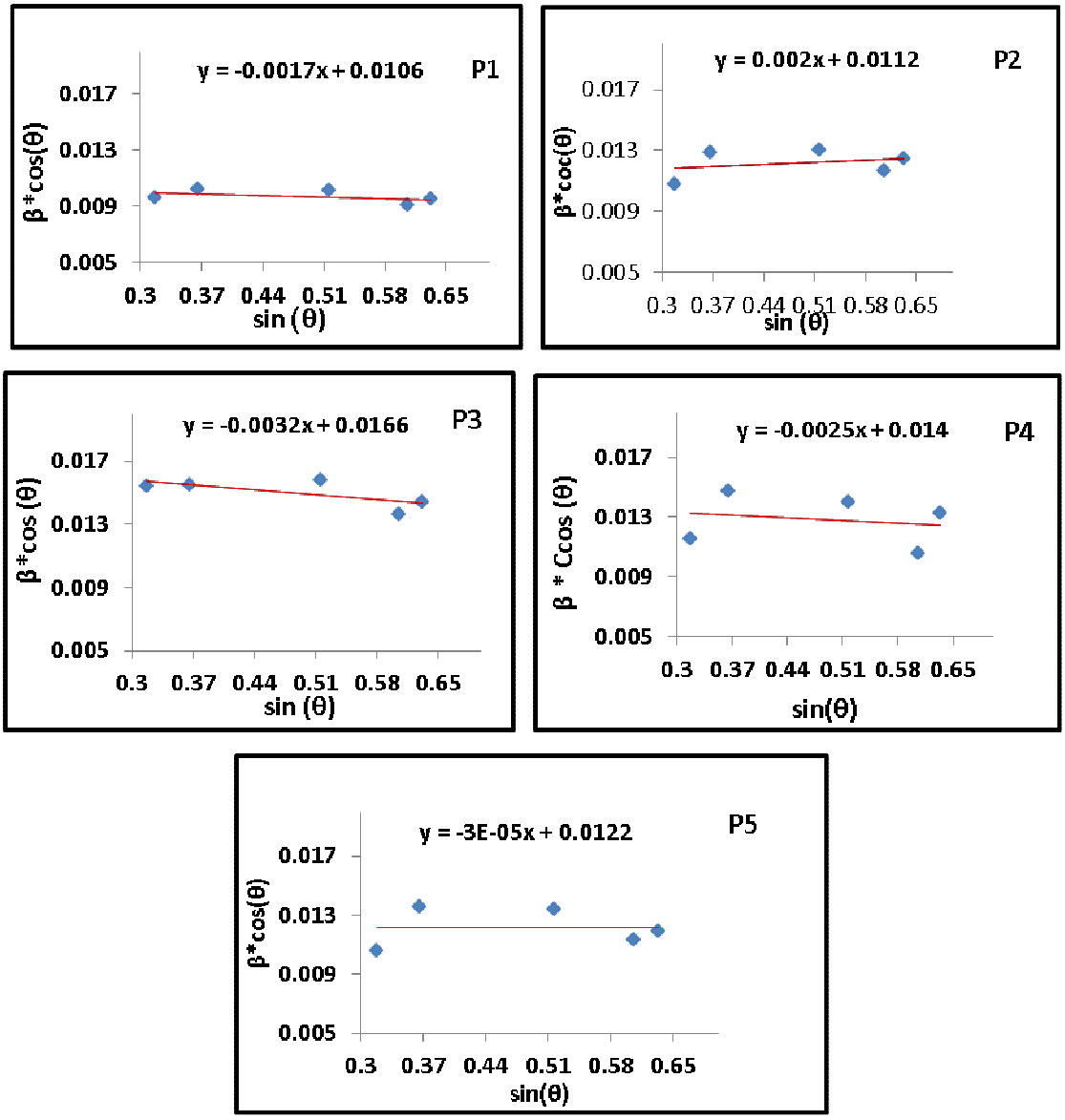

Figure 3. Williamson Hall plot of MgO-NPs.

Particle size and Strain are accounted from the slope and y-intercept of the appropriate line respectively. From the lattice parameters accounts it was noticed that this strain may be attributed to the lattice contraction. It is plotted with sinΘ on the x-axis and $\beta_{hkl}\cos\Theta$ on the y-axis (β_{hkl} in radian). Table (1) shows strain and crystallite size according to Williamson-Hall and Scherrer for MgO nanoparticles.

Table 1. Strain and crystallite size according to Williamson-Hall equation and Scherrer of MgO-NPs

Samples	Molar ratio (Nitrate: Citric acid) M	D_{Sh} (nm)	D_{W-H} (nm)	Micro Strain(ε) $*10^{-3}$
P_1	1:0.5	13.55	14.26	-0. 425
P_2	1:0.6	10.79	11.47	0. 5
P_3	1:1	8.94	9.29	-0. 8
P_4	1:1.75	9.38	10.96	-0. 625
P_5	1:2	10.19	11.49	-0.0075

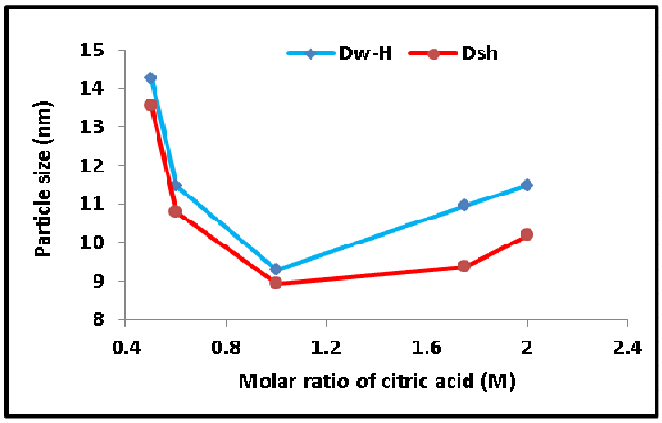

Figure 4. the difference between the grain size calculated from equation (Debye-Scherrer) and equation (Williamson - Hall).

3.2. lattice parameter (a)

The lattice parameter of individual composite was calculated by using the equation (K. Rama Krishna, K. Vijaya Kumar, & Dachepalli Ravinder . 2012).

$$d_{hkl} = \frac{a}{\sqrt{h^2 + k^2 + l^2}} \quad \ldots (3)$$

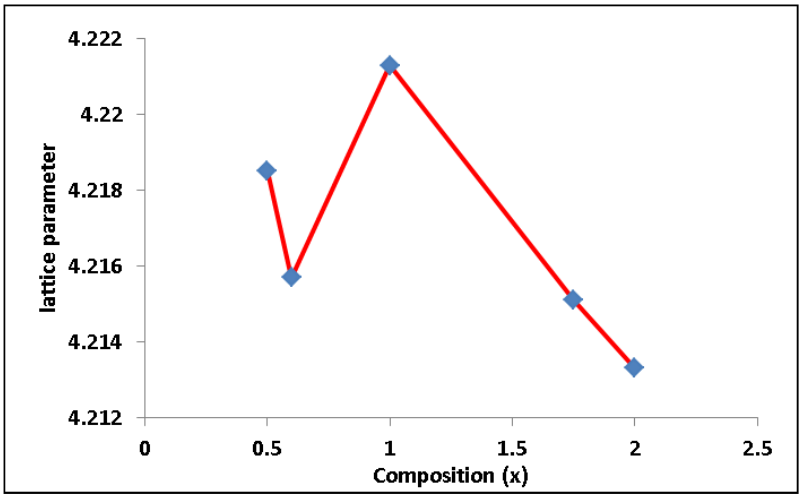

Figure 5. Variation of lattice parameter with composition.

Figure 5 Showing that the lattice of the sample fixed rate (P_5) is the best value when compared with cards (JCPDS Card) standard, but was also observed that a fixed rate lattice least when increasing the concentration of citric acid is due to because of generated stress, which leads to compression of the lattice**.**

3.3. SEM images analysis

The SEM micrographs for MgO-nanoparticle (P_1, P_3 and P_4 are exhibit in figure (6).

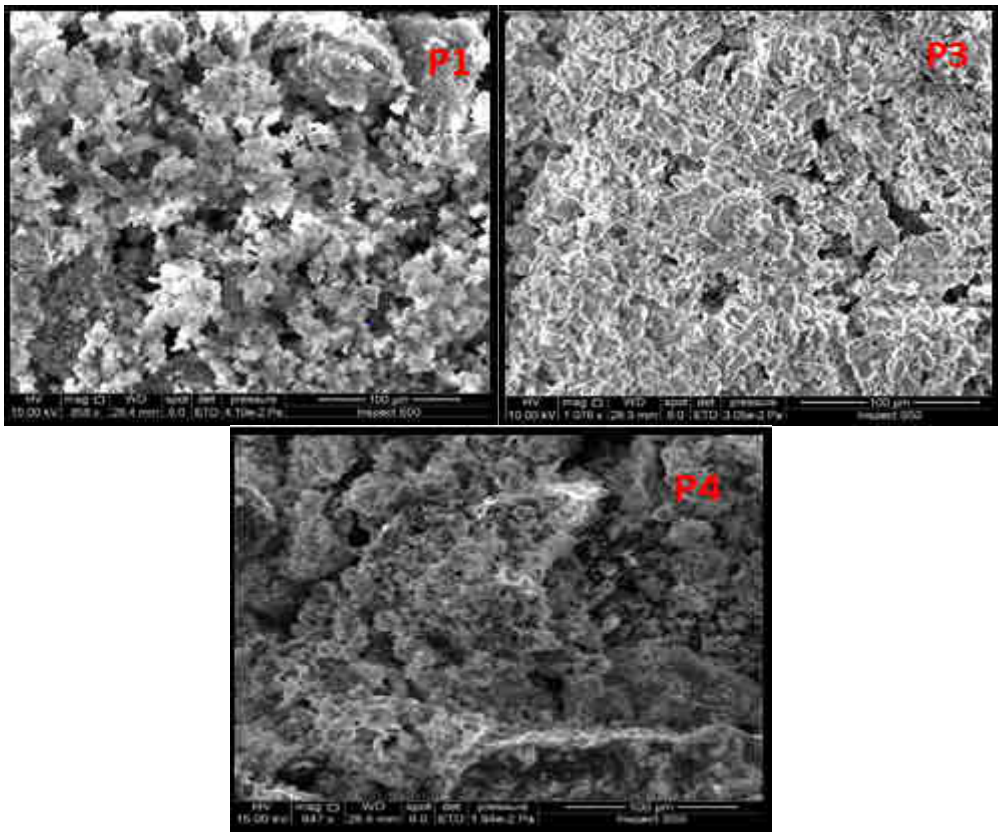

Figure 6.. SEM images of MgO nanopowders at different fuels of glycine, urea, and thiourea fuels at three different molar ratios P_1) 1:0.5, P_3) 1:1 and P_4)1: 1.75 .

The SEM images for MgO powder prepared with fuel (Citric acid) at three various molar ratios are exhibit in Fig. 6. The morphology of the oxides is mostly spherical with some agglomeration.

3.4. Texture Coefficient (TC)

The texture coefficient (TC) idealizes the texture of the particular plane, diversion of which from unit denotes the favored growth. Quantitative informations suspends the favoritism crystallite vectoring was getting from the varied texture coefficient (TC) defined as (Ziad T. Khodair, Asaad A. Kamil, Yamamah K .Abdalaah . 2016).

$$Tc_{hkl} = \frac{I_{hkl}/I_{o\,hkl}}{\frac{1}{N}\sum_{N} I_{hkl}/I_{o\,hkl}} \qquad \ldots\ldots(4)$$

where, *Io(hkl)* is the standard intensity of the plane *(hkl)*, I(hkl) is the measurable relative intensity of a plane *(hkl)*, *n* is the number of diffraction peaks and *N* is the reflection number . A sample with randomly directed crystallite presents texture coefficient TC_{hkl} equates (1), while the bigger this value, the bigger abundance of crystallites directed at the *(hkl)* direction. The counted texture coefficient TC_{hkl} are antedated in Table 2. It can be seen that the highest texture coefficient TC_{hkl} was in (2 2 0) plane for MgO nano powder

Table 2. The X-ray diffraction data results of the crystalline MgO nano powder.

Samples	$Tc_{(200)}$	$Tc_{(220)}$	$Tc_{(222)}$
P_1	0.91477	1.07896	1.00625
P_2	0.91477	1.07896	1.00625
P_3	0.92930	1.04845	1.02223
P_4	0.92930	1.04845	1.02223
P_5	0.90838	1.00155	1.09006

4.0. Optical measurements

In order to study the optical attributes of nanoparticles, was dissolved (0.025M) of nano powder in 5ml of double distilled water, then put the solution in ultrasound for 5 minutes . A reference sample and the weakness of the water sample extraction and magnesium oxide, which was dissolved in double distilled water, placed in the absorption spectrometer. This action is to delete the absorption of water and absorption of nanoparticles Account. The absorbance spectra of magnesium oxide nanoparticles are depicted for all fuel ratios. Show fig. (7) the absorbance which decreased when the length wave is increasing. The highest absorbance at the short wave length mainly attributed to the that the fallen photon unable to tease the electron and moved it from valence pack to connect pack because of the energy of the fallen photon lease than the energy of gap to the energy of semiconductor. The levels of energy between valence pack to connect pack which absorb the photons with the lowest energy. So the absorbance was diminished when the length wave is increasing It indicates that the absorption positions depend on the morphologies and nanoparticle of MgO (Tariq.A.Al-Dhahir , & Karrar Ameen Alsoltani. 2015). Majid Farahmandjou & Mahsa Zarinkamar. 2015).

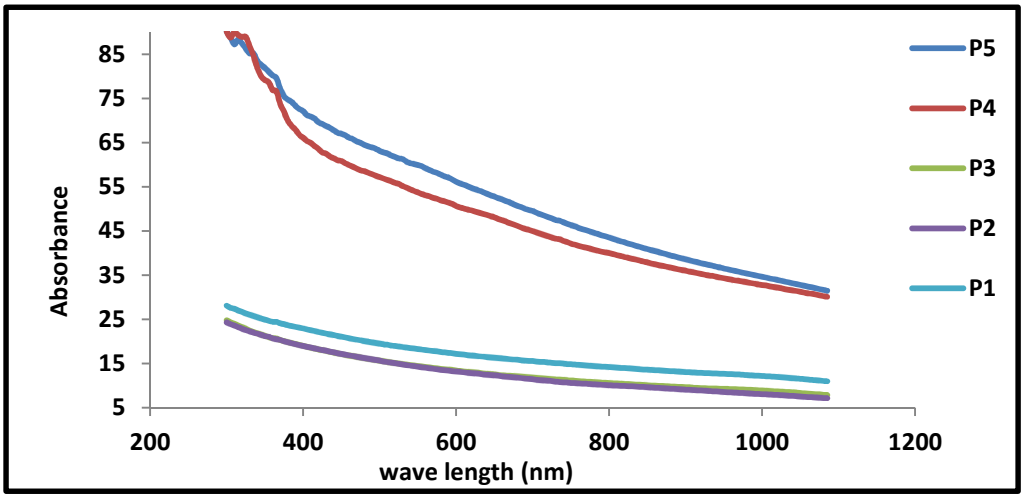

Figure. 7. UV–Vis absorption spectra of MgO nanoparticles.

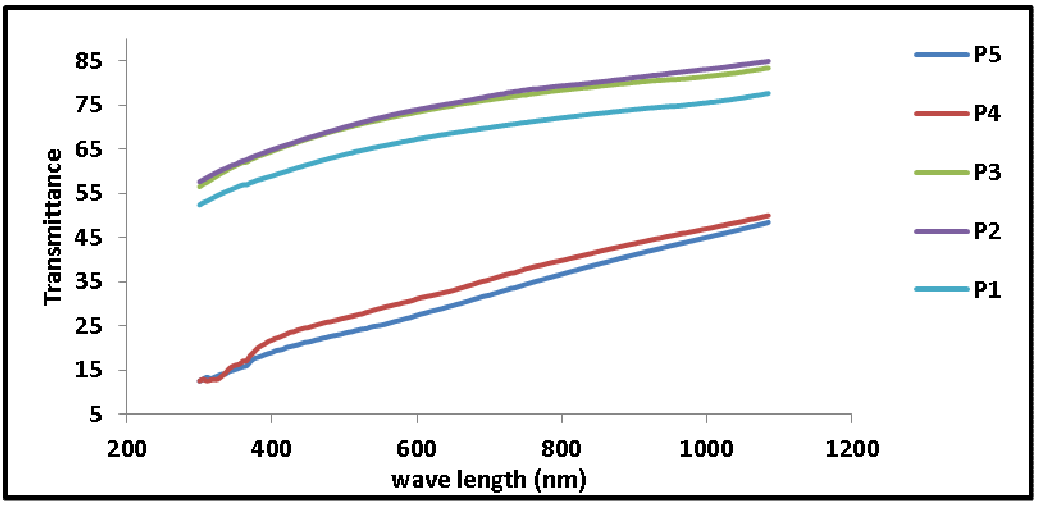

Figure 8. UV–Vis Transmittance spectra of MgO nanoparticles.

A plot is drawn between wave length and Transmittance, the resulting plot was shown in Fig. (8). From the plot it is observed that for all the samples the transmittance decrease with increase in fuel amount mainly attributed to the increase in the amount of fuel leads to increased donor levels near the conduction package, so be ready to receive the electrons so will increase the possibility of absorption of photons with a high proportion of low-lying energy and thus will increase the absorption and less permeable.

5. Conclusions

MgO nano-particles were prepared by auto-combustion process using magnesium nitrate Mg($NO_3)_2$. 6(H_2O) and citric acid ($C_6H_8O_7$. H_2O) as fuel, modes diffraction of x-ray (XRD) to the produced samples that the tops will becomes stronger and sharper when fuel ratio (1:0:5 M) (fuel : salt) . which refers that MgO crystalline are better naonocrystalline size, and the crystallized. The SEM images for MgO powder prepared of the show morphology of the oxides is mostly spherical with some agglomeration. The highest absorbance at the short wave length mainly attributed to the that the fallen photon unable to tease the electron and moved it from valence pack to connect pack because of the energy of the fallen photon lease than the energy of gap to the energy of semiconductor. The levels of energy between valence pack to connect pack which absorb the photons with the lowest energy. So the absorbance was diminished when the length wave is increasing It indicates that the absorption positions depend on the morphologies and nanoparticle of MgO. The transmittance was increased when the length waves were increased , attributed to the increase in the amount of fuel leads to increased donor levels near the conduction package , So be ready to receive the electrons so will increase the possibility of absorption of photons with a high proportion of low-lying energy and thus will increase the absorption and less permeable.

References

Jiahai, B. Fantao, M. Chuncheng, W. Yunxia, Z. Huihui, T. & Juncheng, L. (2011).Solution combustion synthesis and characteristics of nanoscale MgO powders. Journal of Ceramics – Silikáty, 55(1), 20-25.

G. Dercz, K. Prusik, L. Pajaki , R. Pielaszek , J. J. Malinowski , & W. Pudlo.(2009). Structure studies on nanocrystalline powder of MgO xerogel prepared by the sol-gel method . Journal of Materials Science-Poland, Vol. 27(1), 202-207.

V. S tengl , S. Bakardjieva, M. Mar kova , P. Bezdic ka, & J. S ubrt .(2003). Magnesium oxide nanoparticles prepared by ultrasound enhanced hydrolysis of Mg-alkoxides. Journal of Materials Letters, 57, 3998 – 4003.

Zhen-Xing Tang , & Lu-E Shi. (2008). Preparation of nano-MgO using ultrasonic method and its characteristics. Journal of Ecletica Quimica, 33(1) 15 – 20.

G. Mahmoudzadeh, S. A. Khorrami, S. S. Madani & M. Frounchi .(2012). The influence of different fuel additives at different molar ratios on the crystallite phase formation process, structural characteristics and morphology of dispersed zinc ferrite powders by sol-gel auto combustion . Journal of Ceramic Processing Research. 13(4),368-372.

Y. T. Prabhu, K. Venkateswara Rao, V. Sesha Sai Kumar, & B. Siva Kumari. (2013). X-ray Analysis of Fe doped ZnO Nanoparticles by Williamson-Hall and Size-Strain Plot. Journal of Engineering and Advanced Technology (IJEAT), 2, 268-274.

Nabeel A. Bakr, Ziad T. Khodair & Israa A. Alghalabi. (2015). Effect of co doping on structural and optical properties of ZnO thin films prepared by chemical spray pyrolysis. Journal of Current Research, 7 (2), 12411-12417.

M. J. S. Mohamed, & N. Selvakumar, (2012). Effect of Strain in X-ray Line Broadening of MoSi2-10% SiC Ceramic Nanocomposites by Williamson Hall Method,79(1), 82-88 .

K. Rama Krishna, K. Vijaya Kumar, & Dachepalli Ravinder .(2012). Structural and Electrical Conductivity Studies in Nickel-Zinc Ferrite. Journal of Advances in Materials Physics and Chemistry, 2, 185-191.

Ziad T. Khodair, Asaad A. Kamil, Yamamah K .Abdalaah .(2016).Effect of annealing on structural and optical properties of $Ni_{(1\_x)}Mn_xO$ nanostructures thin films. . Journal of Physica B: Physics of Condensed Matter, 503, 55-63.

Tariq.A.Al-Dhahir , & Karrar Ameen Alsoltani. (2015). Effect of Doping by Mg on the Optical and Structural Properties of SnO2 Nanoparticles. Journal of Advanced Research in Science Engineering and Technology, 2, 857- 863.

Majid Farahmandjou & Mahsa Zarinkamar. (2015). Synthesis of nano-sized ceria (CeO_2) particles via a cerium hydroxy carbonate precursor and the effect of reaction temperature on particle morphology. Journal of Ultrafine Grained and Nanostructured Materials, 48, (1), 5-10.